

Supplementary Information published Online for the paper entitled:

Modeling study on the Air Quality Impacts from Emission Reductions and Atypical Meteorological Conditions during the 2008 Beijing Olympics

Jia Xing^{1,2}, Yang Zhang², Shuxiao Wang¹, Xiaohuan Liu³, Shuhui Cheng³, Qiang Zhang⁴,
Yaosheng Chen², David G. Streets⁴, Carey Jang⁵, Jiming Hao^{1, *}, Wenxing Wang³

¹ Department of Environmental Science and Engineering, and State Key Joint Laboratory of Environment Simulation and Pollution Control, Tsinghua University, Beijing 100084, CHINA

²North Carolina State University, Raleigh, NC 27695, U.S.A.

³Shandong University, Jinan, Shandong Province, 250100, P.R. China

⁴Argonne National Laboratory, Argonne, IL 60439, U.S.A.

⁵The U.S. Environmental Protection Agency, Research Triangle Park, NC 27711, U.S.A.

1. Description of emission inventory

The gridded emission data used for CMAQ simulations at horizontal grid resolutions of 36-km and 12-km simulations are provided by the Argonne National Laboratory (ANL), which was developed by extrapolating the 2006 activity data to the year 2008 using the “top-down” method described by Zhang et al. (2009a) and by updating those reported by Streets et al. (2006) and Zhang et al. (2007a, b). The use of these emissions, however, for simulations at 4-km will cause large errors because of a lack of local information on spatial distributions of emission sources. For nested CMAQ simulations at 4-km, local “bottom-up” emission datasets are therefore implemented based on a detailed study at Tsinghua University (Wang et al. 2010a). These bottom-up emissions are more accurate than the top-down emissions, because they are aggregated from emissions of thousands of individual power plants, factories, and heating boilers, with higher accuracy in spatial distribution of important sources. In addition, certain emission reductions affected by staged control policies were quantitatively evaluated after thorough assessments, and its accuracy has been

* Corresponding author: Ji-Ming Hao, hjm-den@tsinghua.edu.cn; Tel: 86-10-62782195, Fax: 86-10-62773650

validated through comparison with environmental monitoring data (Wang et al., 2010a). After considering the air pollution control measures taken during August 2008 Olympics, combined with the Beijing Staged 14th air quality controls (<http://www.bjepb.gov.cn/bjhb/publish/portal0/tab151/info15394.htm>), total emissions of SO₂, NO_x, PM₁₀ and non-methane volatile organic compounds (NMVOC) in Beijing were reduced by -58%, -56%, -52%, and -59%, respectively, in August 2008, as compared to emissions in August 2007. As shown in Figure S1, relative to emissions in 2007, the emission reduction in 2008 concentrated in several areas. The 4km domain-averaged percentage emission reduction of SO₂, NO_x, PM_{2.5} and NMVOC are relatively small (i.e., -2%, -11%, -9% and -7% respectively). More details on the emissions used in this study can be found in Wang et al. (2010a) and Zhao (2009).

In this study, local “bottom-up” emission datasets are implemented based on a detailed study at Tsinghua University. For large point sources (e.g., power plants), we use the point-source module of Sparse Matrix Operator Kernel Emissions (SMOKE) Model (<http://www.smoke-model.org/index.cfm>) to calculate plume heights from stack height, stack diameter, exhaust temperature and exhaust velocity of sources, and allocate emissions to vertical layers. For other area sources (emission height is less than 30m), we just simplified allocate all the emissions amounts to the surface layer in the model. Biogenic emission was calculated by MEGAN (Guenther et al., 2006).

Due to the aforementioned discrepancies in the sources of emissions at 4-km and at coarser grid resolutions, the result analyses were performed for simulations over the 4-km domain, which used initial and boundary conditions (ICs and BCs) derived from the 12-km simulations. For 2008ACT and 2008HYP simulations at 4-km, we used the same ICs and BCs derived from the

12-km simulations for August 2008 with gridded emissions from ANL. Similarly, 2007ACT and 2007HYP simulations at 4-km use the same ICs and BCs derived from the 12-km simulations for August 2007. We modified ANL's 2008 emissions at 36-km and 12-km over the Beijing area to get 2007 emissions, but keep emissions in other regions the same as 2008.

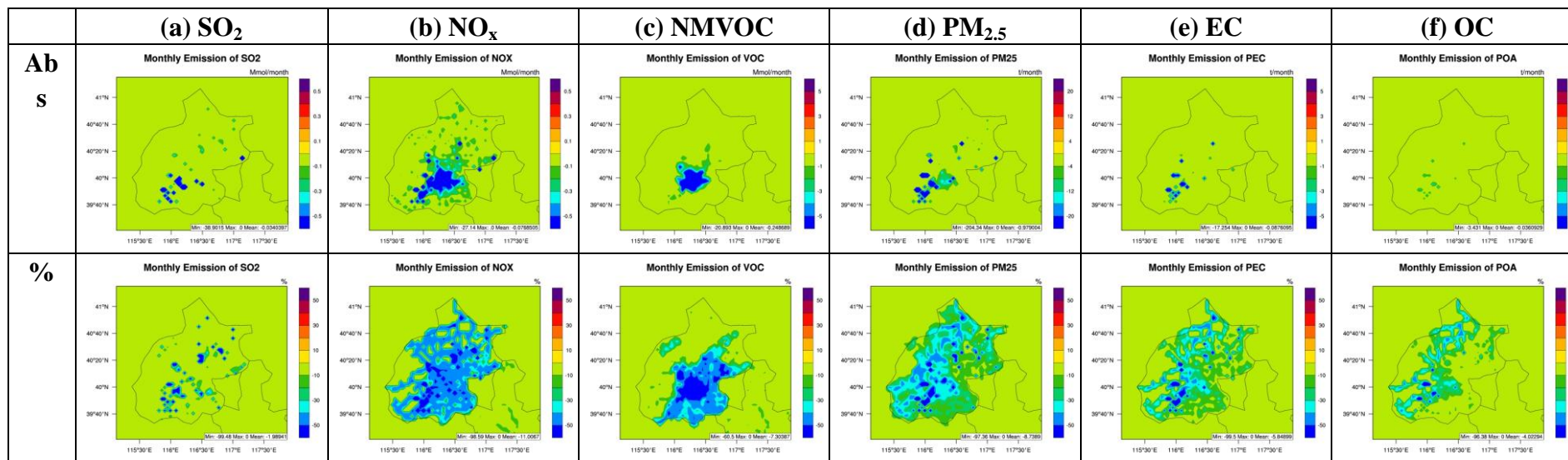


Fig. S1 Spatial distributions of the differences between the gridded emissions in August, 2007 and 2008 (Abs: 2008 minus 2007; %: Abs divided by 2007).

2. Performance Evaluation for August 2007/2008 Baseline Simulations and Uncertainties

Table S2 summarizes the observational data used for model evaluation in this study. The variables include surface concentrations of SO₂, NO₂, and PM₁₀ using observational data derived from the Air Pollution Index (API) for Beijing city (Jiang et al., 2004). O₃ mixing ratios and concentrations of PM_{2.5} and its species are compared with observations in the two sites monitored by Tsinghua University: Tsinghua Campus site (THU) and Miyun site (MIY). Satellite retrievals are used to evaluate the column mass abundance of NO₂, SO₂, CO, Tropospheric Ozone Residual (TOR) and AOD following the same method of Zhang et al. (2009b). Meteorological parameters including temperature, relative humidity (RH), wind speed (WSP), and wind direction (WDR) are compared with observations from 20 surface monitor sites in Beijing. The statistical measures calculated include the normalized mean bias (NMB) and the normalized mean error (NME), and their definitions are provided by Zhang et al. (2006).

Table S3 gives statistics of model performance at 4-km over Beijing Area from August 2007/2008 baseline simulations (2007ACT and 2008ACT). Model reproduces well 2-m temperature (T2) in both August 2007 and August 2008 and 2-m relative humidity (RH2) in August 2008, with a moderate underestimation by 24% on RH2 in August 2007. The ranges of NMBs and NMEs are from -24% to 5% and from 17% to 38%. Model overpredicts wind speed at 10-m (WSP10) by 19% in both months, and the NMEs are 55% and 61% for 2007 and 2008. The NMBs for wind directions at 10-m (WDR10) are small (-7% to 6%) but the corresponding NMEs are relatively large (48% to 51%), indicating error cancellation in NMBs. MM5 performs poorly for precipitation amounts, with NMBs and NMEs of -77% to 15%, and 51% to 77%, respectively. The large bias in precipitation predictions may be mainly caused by limitations in the Kain–Fritsch cumulus scheme and the

Reisner 1 cloud microphysical parameterization in representing clouds and precipitation.

Predicted surface NO₂ concentration is comparable with observations in 2007, with NMB and NME of 12% and 20%, respectively. More than 40% overprediction occurs in surface NO₂ concentration predictions in August 2008, probable due to uncertainties of spatial distributions of NO_x emissions, as well as the emissions of VOC which is involved in the oxidation process of NO₂ to NO₃⁻. Another source of errors may be due to the comparison of the simulated grid-average values with pointwise observational data derived from API. Such an overprediction, however, cannot be seen from the column comparison with the OMI satellite. Model reproduces NO₂ column densities well for both months. The ranges of NMBs and NMEs are from -8% to 12% and 18% to 20%. SO₂ concentrations and column densities are higher by a factor of 3 comparing to surface and satellite observations, respectively. Given the lower SO₂ level in summer, the impact of the uncertainties from the spatial distribution of emission sources and temporal variation caused by the time-factors of seasonal variations in heating plants on simulated SO₂ concentrations is enlarged (Wang, 2006), leading to significant overpredictions. Besides, the underestimate of aqueous-phase oxidation of SO₂ to form SO₄²⁻ is another probable reason to explain the bias. Day-to-day variations of surface O₃ in August 2008 were validated by Wang et al., (2010a). The NMB and NME of daily afternoon mean O₃ in MIY are 9% and 25%. TOR and Tropospheric CO column densities are moderately underpredicted, with NMBs of -27% to -19%. Uncertainties from regional emissions of precursors, upper layer boundary conditions, as well as biases in simulated meteorological conditions may contribute to such discrepancies.

Moderate overpredicitons or underpredictions occur in surface concentrations of PM₁₀ and PM_{2.5}, with NMBs and NMEs of -15% to 28% and from 37% to 67%, respectively. Compared with

measured PM_{2.5} species concentrations at THU, the ranges of NMBs and NMEs for SO₄²⁻, NO₃⁻, and NH₄⁺ are -28% to 57% and 70% to 103%. The overpredictions of SO₂ concentrations but underpredictions of SO₄²⁻ concentrations in 2008 may indicate the underestimate of aqueous-phase oxidation of SO₂ to form SO₄²⁻ due to inaccurate cloud predictions and underestimation of RH. Ammonium is moderately overestimated by 57%. Observed degree of sulfate neutralization (DSN) is less than 2 indicating NH₃-limited chemical regime, while simulated DSN is close to 2. Uncertainty of spatial distributions of NH₃ emission may help explain such a bias. Concentrations of elemental carbon (EC) and organic carbon (OC) are moderately underpredicted by 17% to 45%. Such biases may come from the uncertainty of primary emissions for EC, as well as the model deficiency in simulating secondary organic aerosols (SOA) for OC. In particular, the ratio of simulated SOA to total organic aerosols is less than 5% at THU, which is much lower than that reported in Pandis et al. (1992); Castro et al. (1999) and Duan (2005) (i.e., 15-70%). Compared with satellite, AOD is overpredicted by 32% in August 2007 and 83% in August 2008. Uncertainty of regional emissions of BC and OC emissions, and the retrieval errors of MODIS products may contribute to this bias.

The statistics indicate that the model generally catch the meteorological conditions and pollution concentrations. First, the model can reproduce the atypical meteorological conditions, i.e., decrease of temperature, increase of relative humidity, more precipitations from 2007 to 2008. Therefore the sensitivity study on the Met-driven impacts is reasonable. The changes of pollutant concentrations as well as PA results in two different meteorological conditions are able to reflect the Met-driven impacts and its mechanism. Secondly, the model has good reproducibility of inter-annual changes for primary pollutants, i.e., surface concentration of NO₂, SO₂, PM₁₀, EC, and

column densities of NO₂, SO₂, CO. The model simulations are consistent with the observations, which confirm the significant impact of emission reductions. The differences of pollutant concentrations and PA results between controlled and uncontrolled emission scenarios reflect the effectiveness of emission controls. These results are consistent with that given by Wang et al. (2010a) and Wang et al. (2009b).

For secondary pollutants which dominated by both meteorology and emissions, the inter-annual changes are not well reproduced as that for primary pollutants, since they're suffering the uncertainties from meteorological field, emissions, and the model's atmospheric chemistry. For example, the simulated change of PM_{2.5} (-4%) is not as much as the observed one (-19%). Slightly underestimation of RH (by 6-20%) may cause the underestimation (by 28%) of aqueous-phase oxidation of SO₂ to form SO₄²⁻. Uncertainty of spatial distributions of NH₃ emission may explain the moderately overestimation of ammonium (by 57%). Besides, same as other studies (Han et al., 2008; Hu et al., 2008), the model also suffers the underestimation of the OC concentration (by 35-45%). Because of these limitations, the percentage of Met-driven and Emis-driven impacts from our study have some uncertainties. Therefore we conduct the sensitivity analysis (i.e., Met-driven and Emis-driven) to get the responses of pollutant concentrations and PA results from those two factors. The results indicate that positive effects on pollutants reductions by Emis-driven changes dominate over the entire domain, with the extent of effectiveness from emission reductions varies from locations to locations. The effect of Met-driven changes on species concentrations can be either ways at different locations. Surface concentrations of NO₂, SO₂, O₃, EC, and OC as well as column mass concentrations of NO₂/SO₂/CO in the area of interest are more affected by emissions, while surface concentrations of SO₄²⁻, NO₃⁻, and NH₄⁺, as well as TOR and AOD are more

influenced by meteorology. Such results are consistent with the finding of Wang et al. (2009a,b), Cermak and Knutti (2009), Wang et al. (2010a,b). For PA results, the dominant processes contributing to O_3 , $PM_{2.5}$, SO_4^{2-} , NO_3^- , and SOA are identified through vertical profile and diurnal variations of process contributions. And these results are consistent with the finding of Zhang et al., (2009c) and Liu et al., (2010).

Table S1 Summary of observational dataset for model evaluation used in this study

Datasets	Variables	Type	Frequency	Data pairs	Sites/Spatial Resolutions	Resources
Beijing Meteorological Bureau	T2, RH2, WSP10, WDR10	Meteorology	every 6-hour	2480 in 2007/2008	20 sites in Beijing ^a	Beijing Meteorological Bureau
	Precipitation		monthly total	20 in 2007/2008		
API ^b	SO ₂ , NO ₂	Gaseous species	daily average	31 in 2007/2008	Average of eight sites in Beijing	http://www.bjee.org.cn/api/
Miyun rural site (MIY)	O ₃		daily afternoon average	25 in 2008	Miyun site in the north-east of Beijing (40.48N, 116.78E)	Wang et al., (2010a) and Wang et al., (2009b)
API ^b	PM ₁₀	Particles	daily average	31 in 2007/2008	Average of Beijing monitors	http://www.bjee.org.cn/api/
Tsinghua campus site (THU)	PM _{2.5} , EC, OC		daily average	22 in 2007; 31 in 2008	Tsinghua Campus site(40.00N,116.33E)	Tsinghua University
	SO ₄ ²⁻ , NO ₃ ⁻ , NH ₄ ⁺		daily average	31 in 2008		
OMI	NO ₂ TOR	Vertical Column density	monthly average	Spatial average over urban areas	0.125° × 0.125° 1° × 1.25°	http://www.temis.nl/airpollution/no2.html http://acdb-ext.gsfc.nasa.gov/Data_services/cloud_slice/new_data.html
SCIMACHY	SO ₂				0.5° × 0.5°	http://www.temis.nl/aviation/so2.php
MOPITT	CO				1° × 1°	http://eosweb.larc.nasa.gov/PRODOCS/mopitt/table_mopitt

						.html
MODIS	AOD				$1^{\circ} \times 1^{\circ}$	http://ladsweb.nascom.nasa.gov/data/search.html

^a Meteorological monitoring sites include Shunyi, Haidian, Yangqing, Foyeding, Tangkekou, Miyun, Huairou, Shangdianzi, Pinggu, Tongzhou, Chaoyang, Changping, Zhaitang, Mengtougou, Nanjiao, Shijiangshan, Fengtai, Daxing, Fangshan, and Xiayunling

^b API is the average of monitoring data at 8 sites including Dongsi, Guanyuan, Tiantan, Wanshouxigong, Aoti, Nongzhanguan, Wanliu, and Shijingshan.

API – Air Pollution Index; OMI - the Ozone Monitoring Instrument; SCIAMACHY - Scanning Imaging Absorption Spectrometer for Atmospheric Chartography; MOPITT - the Measurements of Pollution in the Troposphere; MODIS - the Moderate Resolution Imaging Spectroradiometer; T2 – Temperature at 2-m; RH2 – Relative humidity at 2-m; WSP10 – wind speed at 10-m; WDR10 – wind direction at 10-m.

Table S2 Model performance at horizontal resolutions of 4-km over Beijing Area

	August, 2007				August, 2008			
	Obs. ^a	Sim.	NMB	NME	Obs.	Sim.	NMB	NME
Meteorological variables								
Temperature (°C)	25.0	25.7	5%	17%	24.7	24.9	4%	18%
Relative Humidity (%)	69.7	47.8	-24%	38%	76.4	67.0	-6%	28%
Wind Speed (m s ⁻¹)	1.6	1.9	19%	55%	1.6	1.8	19%	61%
Wind Direction (degree)	155.8	145.2	-7%	48%	154.4	163.5	6%	51%
Precipitations (mm/month)	1.5	0.3	-77%	77%	5.1	5.8	15%	51%
Gaseous species								
NO ₂ (ppb)	27.8	30.2	12%	20%	13.4	19.0	42%	44%
SO ₂ (ppb)	4.9	15.2	210%	256%	3.3	10.7	226%	236%
O ₃ (ppb)	No observed data				57.4	56.6	9%	25%
PM and PM species								
PM ₁₀ (μg m ⁻³)	115.2	116.3	14%	37%	72.0	91.9	28%	67%
PM _{2.5} (μg m ⁻³)	74.7	63.7	-15%	45%	60.7	61.1	1%	63%
SO ₄ ²⁻ (μg m ⁻³)	No observed data				19.8	14.3	-28%	96%
NO ₃ ⁻ (μg m ⁻³)	No observed data				10.0	9.1	-10%	70%
NH ₄ ⁺ (μg m ⁻³)	No observed data				5.5	8.7	57%	103%
EC (μg m ⁻³)	6.2	4.2	-32%	35%	3.6	3.0	-17%	37%
OC (μg m ⁻³)	9.1	5.9	-35%	37%	9.0	4.9	-45%	45%
Column densities								
Tropospheric NO ₂ column (1×10 ¹⁵ molecules cm ⁻²)	15.5	17.3	12%	20%	10.3	9.6	-8%	18%
Tropospheric SO ₂ column (Dobson)	0.52	1.61	212%	212%	0.34	1.05	210%	210%
Tropospheric CO column (1×10 ¹⁷ molecules cm ⁻²)	25.9	20.5	-21%	21%	23.8	17.5	-27%	27%
TOR (Dobson)	49.8	40.3	-19%	19%	53.8	41.1	-24%	24%
AOD	0.63	0.83	32%	32%	0.46	0.84	83%	83%

^a The number of data pairs used for calculation is given in Table S1.

3. IPR analysis on PM_{2.5} components (i.e., SO₄²⁻, NO₃⁻ and SOA) in August 2008

PM processes are the dominant source for SO₄²⁻ in the PBL at both sites, and horizontal transport usually acts as a major sink, as shown in Figures S2 a, e. Cloud processes are a small contributor, except for the days when precipitation occurred. PM processes contribute to SO₄²⁻ in all layers as shown in Figure S2 b, and it usually occurs in the afternoon time (Figures S2 c, d) when the atmospheric oxidation ability is sufficiently large to convert S(IV) to S(VI). Horizontal transport and primary emissions are the major source of SO₄²⁻ in the surface layer at THU, whereas vertical transport provides the dominant source for SO₄²⁻ at MIY.

PM processes provide the dominant source for NO₃⁻ in the PBL at both sites, and horizontal transport and cloud processes are the major sinks, as shown in Figure S3 a. As shown in Figure S3 b, the effects of PM processes are different between lower and upper layers. The evaporation of NO₃⁻ usually occurs during afternoon time in the surface layer, as shown in Figure S3 c, then NO₃⁻ from upper layers contribute to the surface layer concentration through vertical transport and mixing. In upper layers the PM processes are the major contributor to NO₃⁻, especially during afternoon (Figure S3 d).

Similar to NO₃⁻, PM processes are the dominant source of SOA in the PBL at both sites, while horizontal transport and cloud process are the major sinks, as shown in Figures S4 a, b. The formation of SOA through PM processes occurs throughout the whole day in the surface layer and during afternoon time in upper layers as shown in Figures S4 c and d.

For SO₄²⁻, as compared to 2008ACT, contributions of emissions and cloud processes at THU, and PM processes at both sites become larger in 2008HYP, along with stronger removal of horizontal transport in the PBL (Figure S2 e). Larger contributions by emissions occur for SO₄²⁻

from 2008HYP in layers 1-2 at THU (Figure S2 f-1), and by PM processes in all layers within the PBL at MIY (Figure S2 f-2). Diurnal analysis shows nearly constant SO_4^{2-} concentrations during one day (in Figures g, h). The net increase in the concentrations of SO_4^{2-} is relatively small, within $1 \mu\text{g}\cdot\text{m}^{-3}\cdot\text{h}^{-1}$ at both sites and in both layers 1 and 7, while positive net-increase value appears during afternoon (at 1-4 pm), indicating contributions from PM processes. Slight increases of SO_4^{2-} concentrations can be found at both sites, especially during nighttime at THU.

In 2008HYP, similar enhancement of PM process contributions and horizontal transport removals to NO_3^- at both sites in the PBL (Figure S3 e). The responses of process contributions of NO_3^- are similar to their original vertical profiles (see Figures S3 f vs. b). Both negative/positive effects of PM processes simulated by 2008HYP in lower/upper layers are enhanced at THU, except negative impacts in lower layers at MIY are weakened since the enhanced atmospheric oxidation capacity favors NO_3^- formation, along with a stronger vertical and horizontal transport that leads to increases in NO_3^- concentrations in all layers (Figures S3 g, h). In the surface layer at both sites, the sharp decrease of net-increase line starts from 7 am (when the inversion layer breaks down), then reaches to the trough at 10 am which indicates the start of NO_3^- evaporation. The peak net-increase occurs at 10 pm at THU, indicating the occurrence of gas-to-particle conversion. Similar peak occurs at around 12 pm in upper layers at both sites.

In 2008HYP, larger PM process contributions to SOA and a stronger horizontal transport removal to SOA at both sites in the PBL (Figure S4 e). The contributions of PM processes are enhanced in all PBL layers (Figure S4 f), along with enhanced vertical and horizontal transport and increase in the SOA concentrations. The peak of the net increase at 12:00 pm at THU (at 3 pm at MIY) in upper layers indicates more intense photochemical reactions and larger SOA formation

rates due to lower temperature and higher RH that favor the formation of SOA.

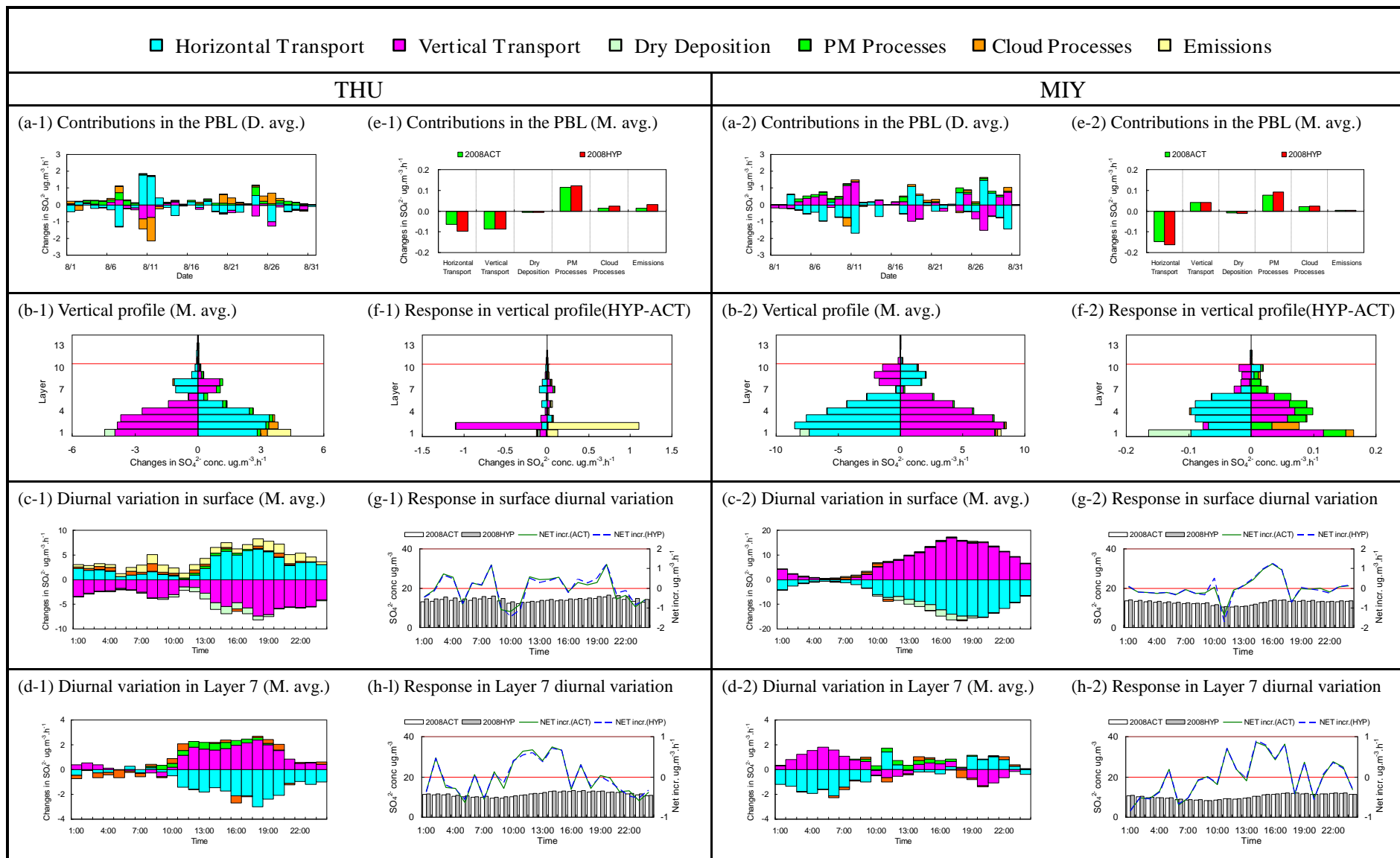


Fig. S2 Integrated processes contributions to SO_4^{2-} mass concentrations in August 2008 (diurnal variations are based on monthly average values over 1:00 to 24:00 Local Time (LT); NET. Incr. is calculated by summing the contributions from all processes; M. avg. = monthly average value; D. avg. = daily average value; The height of layers 1-10 above ground are 36, 72, 145, 294, 444, 674, 1070, 1568, 2093, 2940 meters, respectively)

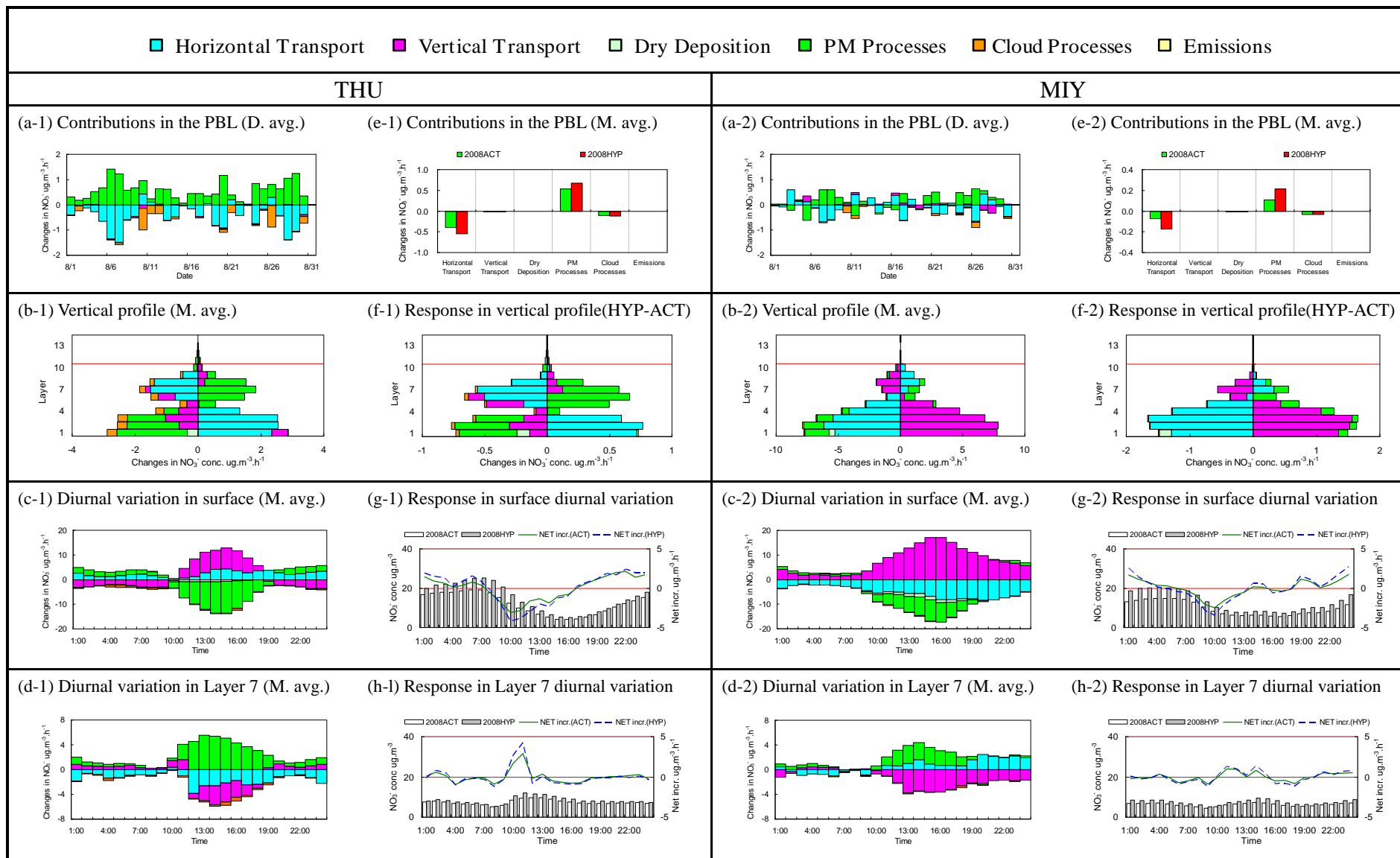


Fig. S3 Integrated processes contributions to NO_3^- mass concentrations in August 2008 (diurnal variations are based on monthly average values over 1:00 to 24:00 Local Time (LT); NET. Incr. is calculated by summing the contributions from all processes; M. avg. = monthly average value; D. avg. = daily average value; The height of layers 1-10 above ground are 36, 72, 145, 294, 444, 674, 1070, 1568, 2093, 2940 meters, respectively)

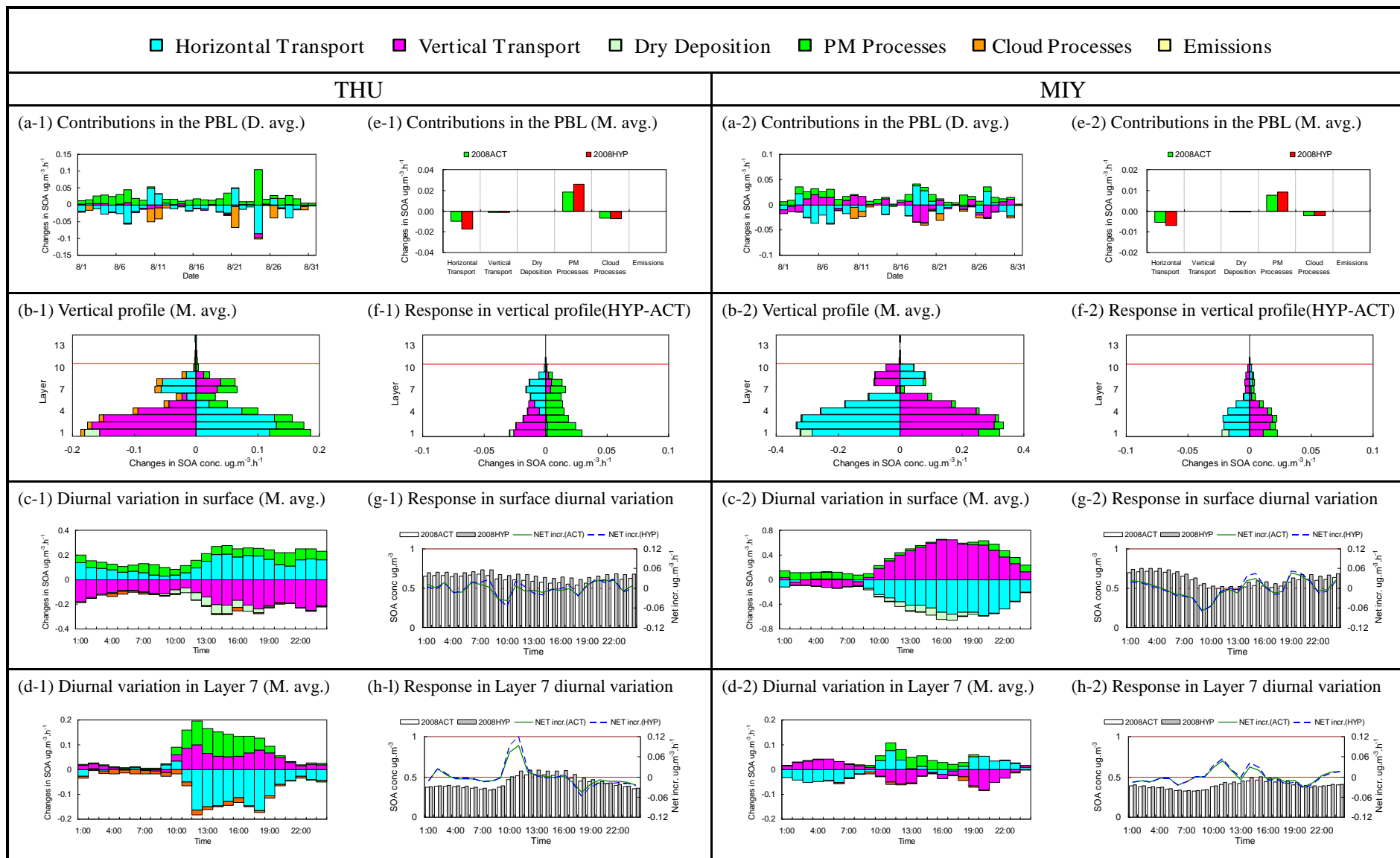


Fig. S4 Integrated processes contributions to SOA mass concentrations in August 2008 (diurnal variations are based on monthly average values over 1:00 to 24:00 Local Time (LT); NET. Incr. is calculated by summing the contributions from all processes; M. avg. = monthly average value; D. avg. = daily average value; The height of layers 1-10 above ground are 36, 72, 145, 294, 444, 674, 1070, 1568, 2093, 2940 meters, respectively)